International Journal of Enhanced Research in Science, Technology & Engineering
ISSN: 2319-7463, Vol. 5 Issue 3, March -2016

SEM study of debonding /pull-out features & FTIR analysis of bonding in fly ash- epoxy particulate composites

Shahad Ibraheem[1], Owen Standard[2], Pramod Koshy[3], Sheila Devasahyam[4], Sri Bandyopadhyay[5]*

[1,2,3,5,] UNSW Australia SMSE; School of Materials Science & Engineering, UNSW Australia;
[4] Federation University of Australia, Ballarat, SITE

ABSTRACT

This research utilises as received coal power fly ash (FA) as a value-added component added to epoxy resin for making a superior matrix for fibre reinforced composites in load-bearing applications. The epoxy resin used in this project was DGEBA cured by cycloaliphatic polyamine at 120 Co for 2 hours. A fly ash with particle size ranging between 2 – 20 micron was added to the epoxy in 0, 10, 20, 30, 40 & 50 wt% proportions. Scanning Electron Microscopy (SEM) of tensile fracture surfaces of the composites using ASTM D638 tensile samples provide significant evidence of Fly Ash debonding and pull-out from the epoxy matrix indicating good mechanical bonding between FA and epoxy matrix. Fourier transform infrared spectroscopy (FTIR) of pure epoxy, pure fly ash and selective composites (20 and40 wt % FA-epoxy composites) shows distinct evidence of fly ash functional groups' interaction with the epoxy matrix. Some selected SIMS (secondary ion mass spectrometry) results are presented for the 20wt % fly ash /epoxy composites.

Keywords: Dispersion, Fly ash (FA), Polymer Matrix Composites (PMCs), Scanning Electron Microscopy (SEM), Fourier Transform Infra-Red spectroscopy (FTIR), Debonding, Pullout.

1. INTRODUCTION

Coal fly ash (FA) is a grey, fine, spherical and lightweight by-product generated in big amounts in thermal power stations. As a 'waste' product, FA is considered to be a very cheap material [1, 2] but it is equivalent or superior to several materials in mechanical / chemical properties like calcium carbonate $CaCO_3$, etc. [3]. FA has numerous useful applications for such as reinforcement in cement/concrete, flowable fill, fly ash bricks/tiles, structural fill/ embankment road base/ sub-base, roofing tiles, paints, mineral fill, blasting grit, mining applications, gypsum panel products, waste stabilization, agriculture, aggregate, and as filler in wood and plastic products [3].

In this work, the matrix chosen was epoxy resin owing to its excellent adhesion to other materials, chemical and heat resistance, good to excellent mechanical properties, and very good electrical insulating properties [4, 5, 6, 7]. Also, epoxy is the most common thermoset plastic for polymer matrix composites (PMC) [4]. Epoxy consists of "dipoxy" short chain polymers often termed as monomer [5], and the hardener is typically a diamine [5, 8]. By curing at elevated temperature [5, 9], the resulting material is a hard substance [4]. During curing, epoxy resins undergo only low shrinkage [typically 2–3%] and do not liberate away any by-products [4].

Reinforcing epoxy polymer with FA helps to improve polymer material properties [10] such as stiffness, mechanical strength, abrasion resistance and chemical durability, and also helps to reduce the total cost [10] and weight [4] of the composite.

However, detailed micro-failure aspects of fly ash in tensile fracture of epoxy – fly ash composite have not been reported in any detail in the literature. Likewise the chemical interaction(s) between fly ash and epoxy has also not been properly established. This paper addresses these two important features of fly-ash epoxy composites and the specific aims of the work are to:

a) Study the tensile fractographic features of FA-epoxy composites as a function of fly ash content of 0, 10, 20, 30, 40 and 50 wt %; and,

b) Determine the effect of FA on the curing behaviour of the composite by Fourier Transform Infrared Spectroscopy (FTIR) of pure cured epoxy, pure fly ash, and two selected composite compositions such as 20 % FA-epoxy and 40 % FA- epoxy. In infrared spectroscopy, IR radiation is passed through a sample. Some of the is absorbed by the sample and some of it is passed through (transmitted). The resulting spectrum represents the molecular absorption and transmission, creating a molecular fingerprint of the sample.

Uncured pure epoxy DGEBA as FTIR peaks as provided in reference [11] shows:

i) 3500 cm $^{-1}$represents O-H stretching.
ii) 3057 cm $^{-1}$ represents stretching of C-H of oxarine ring.
iii) 2965-2873 cm $^{-1}$ bands represent stretching of C-H and CH aromatic and aliphatic.
iv) 1608 cm $^{-1}$ is the stretching in C=C aromatic ring.
v) 1509 cm $^{-1}$ is the stretching in C-C of aromatic.
vi) 1036 cm $^{-1}$ represents the stretching in C-O-C of ethers.
vii) 915 cm $^{-1}$ represent the stretching C-O of oxarine group.
viii) 831 cm $^{-1}$ represent the stretching C-O-C of oxarine group.
iv) 772 cm $^{-1}$ rocking CH_2.

c) To study the mineral distribution and contamination using a highly effective a highly effective Secondary Ion Mass Spectrometry method [9].
d) Energy Dispersive X-ray Spectroscopy, EDS has been used to detect the elements and to compare it with SIMS in direction of how the two methods can detect small amounts of elements [9].

2. EXPERIMENTAL WORK

2.1 Materials:

Diglycidal ether of bisphenol A - (DGEBA) was used as the resin, and cycloaliphatic polyamine was used as a hardener (both supplied by The Barnes, NSW, Australia). The epoxy was a clear liquid having viscosity of 500-1000 mPa.s at 25°C; whilst the hardener's viscosity was 100-300 mPa.s at 25 ^{o}C. Class F fly ash samples were obtained from Tarong power plant Queensland, Australia. Fig 1 (a) shows a Scanning Electron Microscope (SEM) image of the as-received FA at 5000X magnification. The particle size distribution is given in Fig 1 (b).

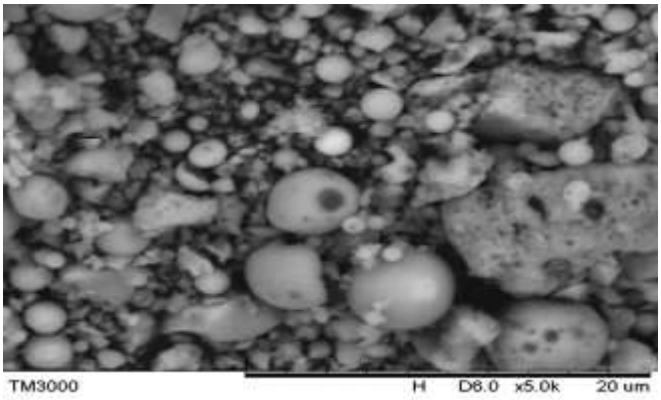

Figure 1 (a): Typical SEM micrograph of raw-as received fly ash.

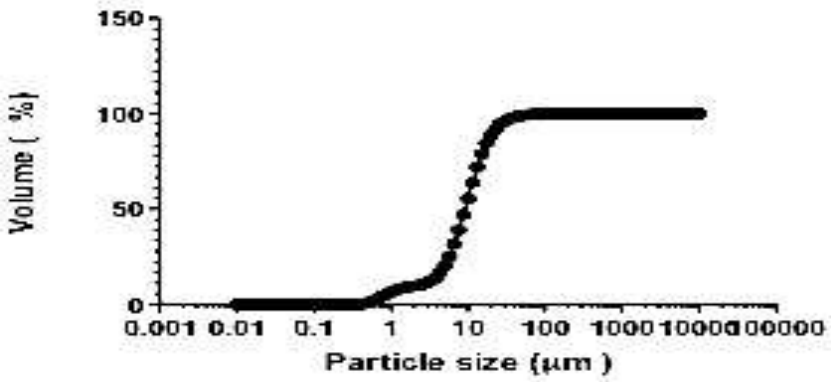

Fig 1 (b): Particle size distribution of as received fly ash using {name the technique}.

The resin and hardener were mixed in 100:50 parts (by volume), then the fly ash was added to the mixture by weight in proportions of 0, 10, 20, 30, 40, and 50 wt% of fly ash in a plastic container by stirring with a rod taking care to minimise the entrapment of air inside the mixture. Tensile specimens were prepared according to configuration specified in ASTM D638 for Type 1 dog bone tensile specimens (see Fig 2). The as-mixed composite was transferred to a dog-bone mould cavity taking care to ensure that the mould cavity was completely filled with and uniformly levelled. Curing was carried out in air at 120°C for 2 hours in an electric oven. The mould was then left inside the oven to cool down slowly to room temperature. Finally, the cured specimens were removed from the mould and cleaned.

2.2 Preparation of Fracture Surfaces:

For each of the six compositions, five tensile test specimens were prepared. Each test specimen was subjected to tensile loading at ~25°C in a tensile testing machine (Instron 5982) using a crosshead speed of 1 mm/min. The specimens were loaded to fracture thus yielding a set of fracture surfaces for examination.

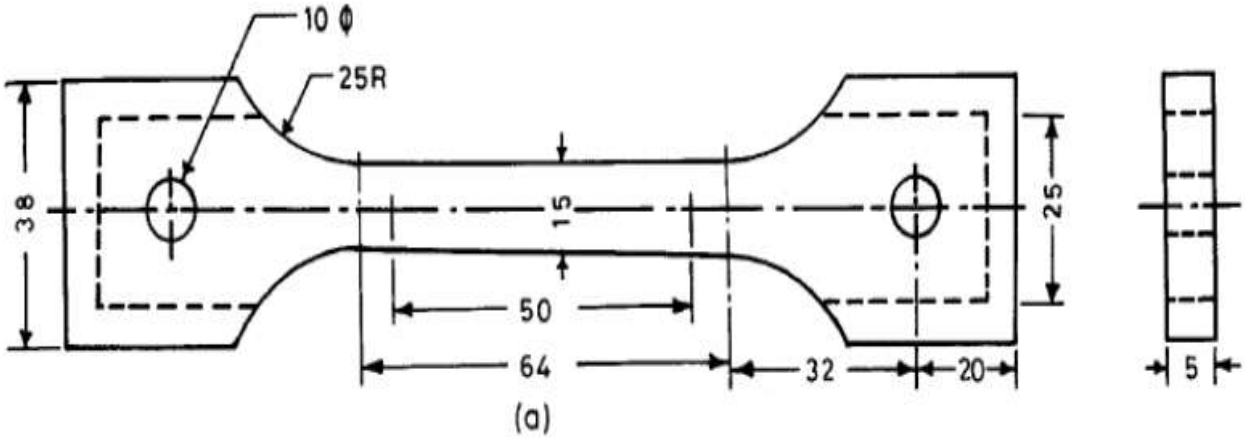

Fig 2: Geometry of tensile test specimen, dimensions in mm (ASTM D 638 Type 1).

2.3. Materials Characterization:
2.3.1. SEM Fracture Morphology of the mechanical test specimens

The fracture surfaces of the tensile test specimens were examined by scanning electron microscopy (TM3000 Table Top, UNSW Australia) Samples, approximately 10 mm x 10 mm x 3 mm, were cut from the tensile specimens (taking care not to damage the fracture surfaces) and the sputter-coated with gold. Fracture surfaces were examined using a range of set magnifications (40X, 800X, 1200X, 1500X, 5000X, and 7000X).

2.3.2. Fourier Transform Infra-Red Spectroscopy (FTIR):

FTIR analysis of pure epoxy, pure fly ash, and two selected composite compositions of 20% FA-epoxy and 40% FA-epoxy were done (PerkinElmer, UNSW Australia) using infrared radiation over a wavenumber range of 1000–650 cm^{-1}.

2.3.3. Secondary Ion Mass Spectrometry (SIMS):

The secondary ion mass spectrometry was done on 20wt% FA-epoxy composite to have an idea on how the fly ash minerals distribute in the epoxy resin and to find out if there is any contamination during the handling of the fly ash till mixing it with epoxy. For sample preparation; the 20wt% FA-epoxy sample was cut to (1cm length, 1cm width, 5cm height). The surface was subject to cleaning by propanol and Decon detergent before analysis. Then, the surface of the tested sample was coated with gold sputter to finally fitted in the special holder ready for testing.

2.3.4. Energy Dispersive X-ray Spectrometry (EDS):

Energy dispersive X-ray spectrometry was done on the surface of unbroken and unpolished tensile specimen for 20wt% FA-epoxy composite.

3. RESULTS AND DISCUSSION

3.1. Scanning Electron Microscopy SEM:

The fracture behaviour of the materials is established by considering the microstructures with increasing magnification. Representative SEM micrographs of the fracture surfaces of the uniaxial tensile samples of pure epoxy and five FA-epoxy composites are shown in figures 3 to 7.

At the magnification of 800X (fig. 3), the following was noted:

- Fig 3a for neat epoxy shows extended vision of fine river marking [17].
- Fig 3b for 10 wt% FA/epoxy composite shows good distribution of the FA particles in the epoxy matrix as well as evidence of FA-epoxy debonding and FA particle pull-out [15].
- Fig 3c for 20 wt% FA epoxy composites shows a more smooth type fracture surface compared to that of the 10 % FA/epoxy material.
- Fig 3d) for 30 wt% FA epoxy composites shows distinct evidence of fly ash particle adherence with the matrix and also there is evidence of some FA particle fracture and some pull-out – indicating strong fly ash [as is evident from FTIR studies as shown in figures below].
- Fig 4f) 50 wt% FA epoxy composite: showing a rather flat brittle fracture surface; some of the fly ash particles remain adhered to the matrix and the others are pulled out which gives better strength to the composite**.**

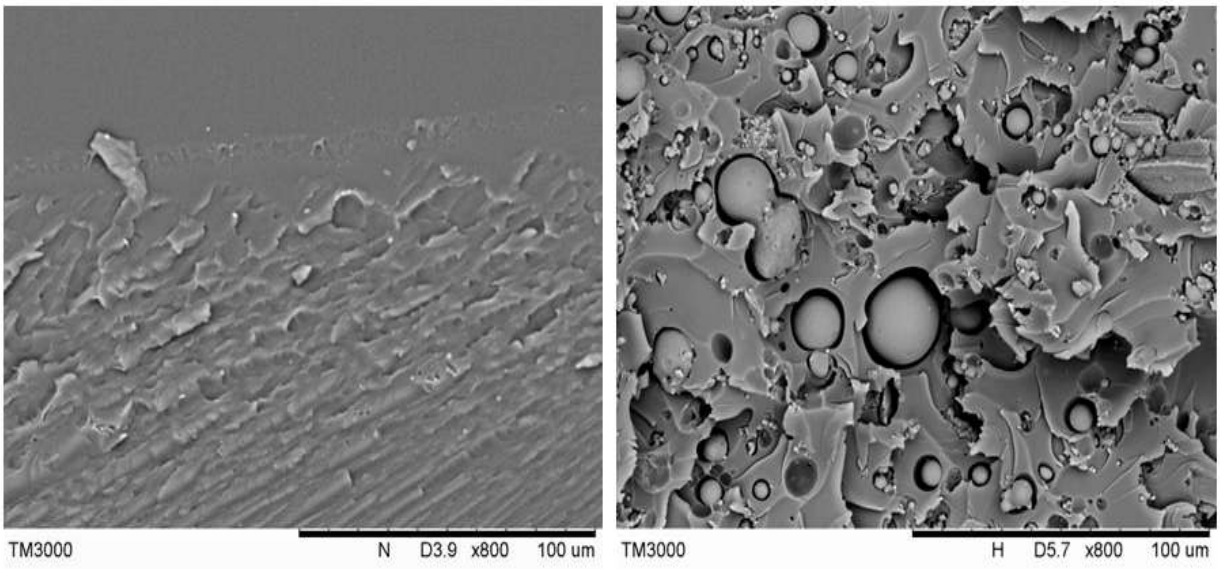

Fig 3; Fig 3; a, b, c, d, e, and f respectively showing SEM images of 0, 10, 20, 30, 40, and 50 wt % FA-epoxy composites under 800 magnification

Left a) Neat epoxy: showing extended vision of fine river marking
Right b) 10 wt % FA: fly ash particles showing predominantly debonding / pull-out

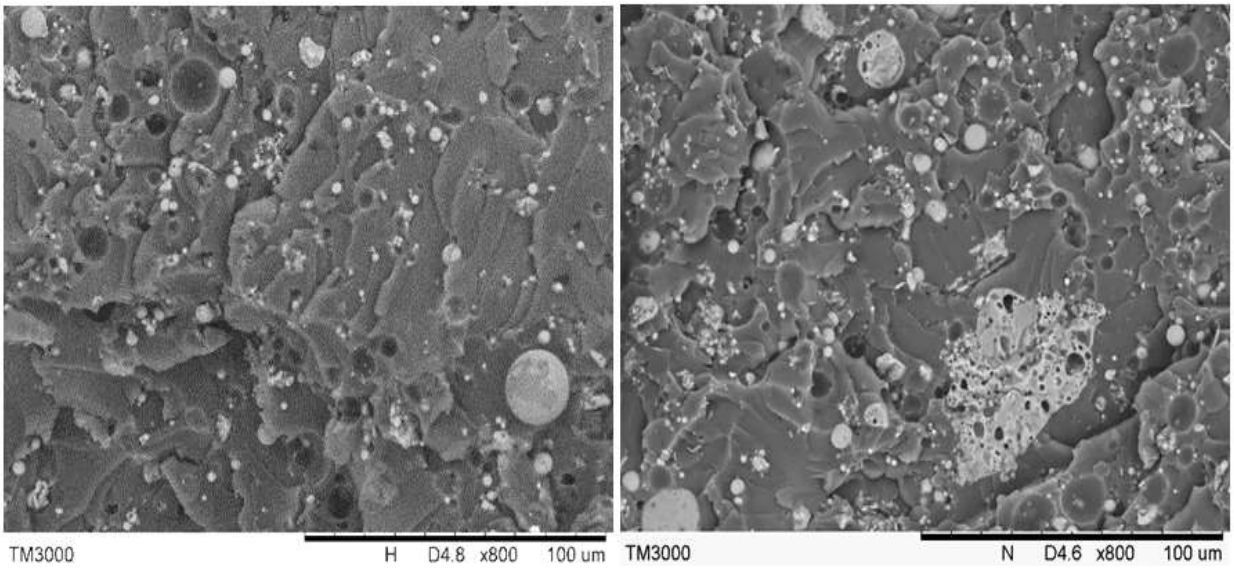

Fig 3; Left c) 20 wt % FA epoxy composites: shows a smoother type fracture surface
Right d) 30 wt % FA composite showing some of the fly ash particles adhered to the matrix and the others are pulled out

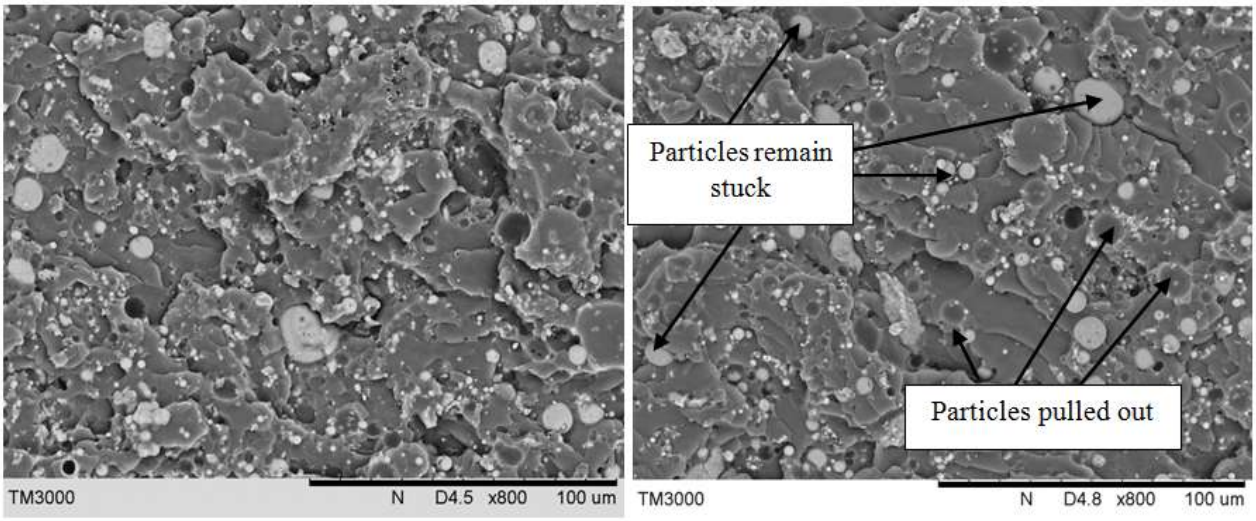

Fig 3; Left e) 40 wt% FA composite: Shows the fly ash particles homogeneously mixed with the matrix, and fractured FA from good bonding ie. lack of pull-out, (the bonding is evident from FTIR studies as shown in figures below.

Right f) 50 wt% FA epoxy composite: Shows a flat brittle fracture surface that some of the fly ash particles remain stuck to the matrix and the others are pulled out which gives better toughness to the composite

At the magnification of 1200X (fig. 4), the following features are noted:

- Fig 4a) of pure epoxy shows obvious and uniform river markings of step - size approximately 12 – 15 microns in width.
- Fig 4b) 10 wt% FA/epoxy**:** shows presence of FA particles significantly preventing the shear deformation of the epoxy [17]; at the same time FA is reducing the shear lip width to typically 5 – 7 micron significantly reducing the ductility and at the same time introducing larger areas of fracture reducing the ductility [17].
- Fig 4c) and d) for 20 wt% and 30 wt% FA-epoxy composites both show FA pull-out which, based on the mechanical behaviour of similar FA-epoxy composites reported elsewhere [15], suggests that the strength and toughness of the composites in this work would be improved relative to pure epoxy.
- Fig 4e) and f) 40 wt% & 50 wt% FA-epoxy composites show that some of the fly ash particles are stuck to the matrix and the others are pulled out; also some fly ash particles are fractured which potentially gives extra toughness due to the energy absorption during debonding and pull-out of FA particles as similar features were observed by other researchers [15]; this microstructure is similar to that at high magnification reported by with other researchers

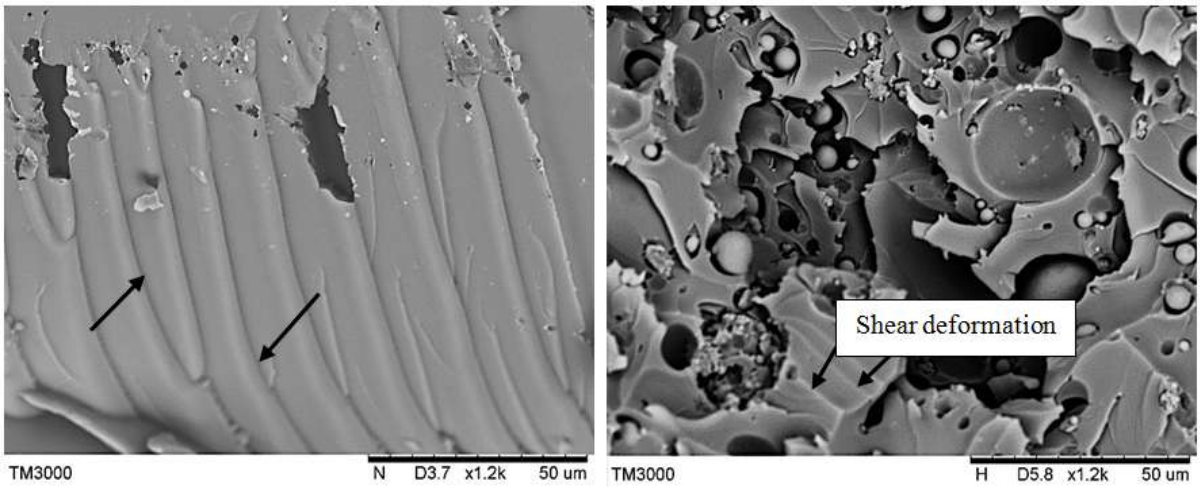

Fig 4; a, b, c, d, e, and f respectively showing SEM images of 0, 10, 20, 30, 40, and 50 wt% FA-epoxy composites 1200 magnification

a) Left: 0 wt% fly ash-pure epoxy, showing nice and uniform shear lip zones of size approximately 12 – 15 microns in width

b) Right: 10 wt% FA: shows presence of FA particles is significantly preventing the shear deformation of the epoxy; at the same time FA is reducing the shear lip width to typically 5 – 7 micron significantly reducing the ductility and at the same time introducing larger areas of fracture reducing the ductility severely

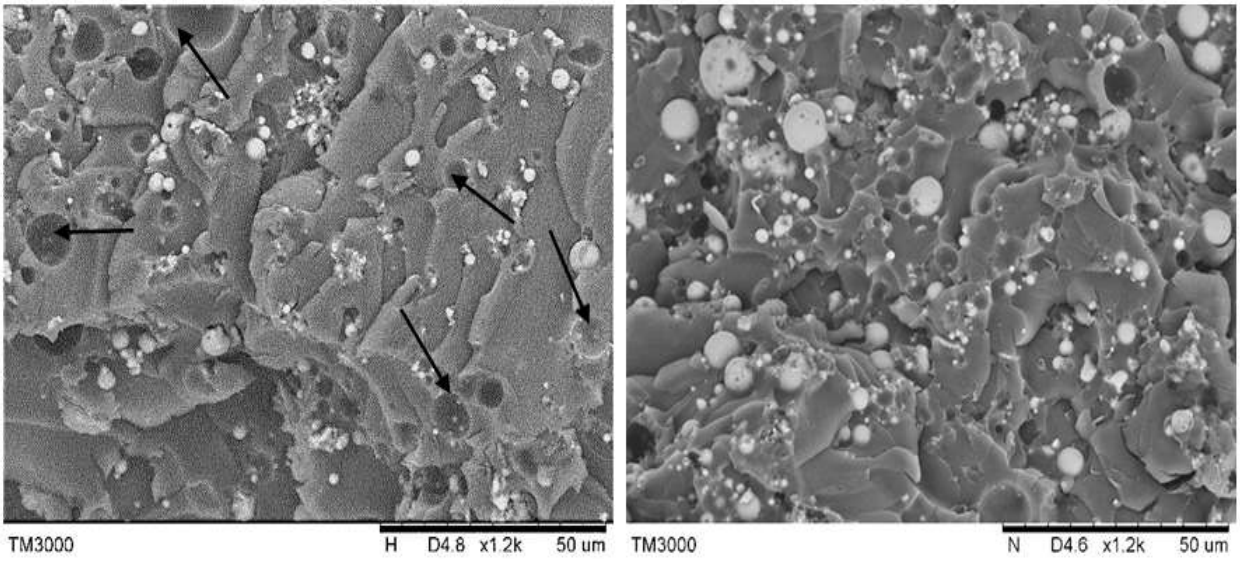

Fig 4; c) Left: 20 wt% FA composites showing FA pull-out (indicated by arrows)
d) Right: 30 wt% FA: Shows the fly ash particles homogeneously mixed with the matrix

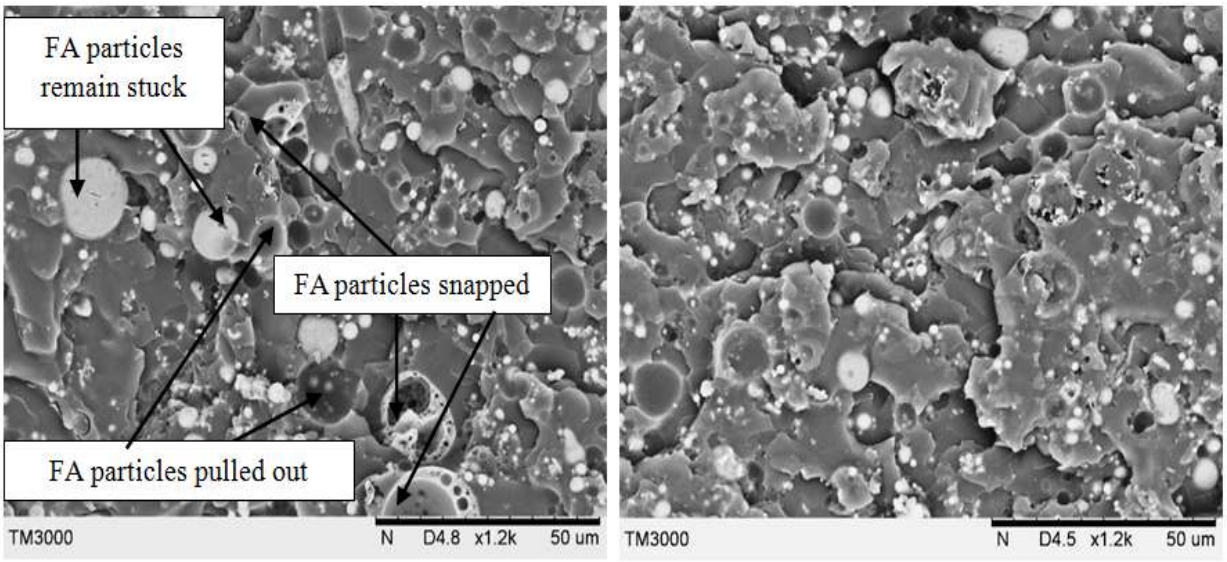

Fig 4; e) Left: 40 wt% FA some of the fly ash particles are stuck to the matrix and the others are pulled out also some fly ash particles snap
f) Right: 50 wt% FA: Shows the fly ash particles homogeneously mixed with the matrix, and some of the fly ash particles remain stuck to the matrix where others are pulled out

At the magnification of 1500X (fig. 5), the following features are observed:

- Fig 5 a) pure epoxy starts showing very small slip (shear) steps with as little as 2 to 5 micron width due to the deformation which happen through the fracture process [17].
- Fig 5 b) 10 wt% FA- epoxy: shows agglomerating of FA and FA fracture.
- Fig 5 c) 20 wt% FA-epoxy composites showing even distribution of FA particles in the epoxy matrix.
- Fig 5 d) 30 wt% FA: Shows epoxy-FA micro-cylinder shell formation and break - out.
- Fig 5 e) 40 wt% FA: Shows mostly even distribution with a small agglomeration from FA particles.
- Fig 5 f) 50 wt% FA: Can easily see substantially FA agglomeration which may offer stress concentration area leading to initiation of a crack [18].

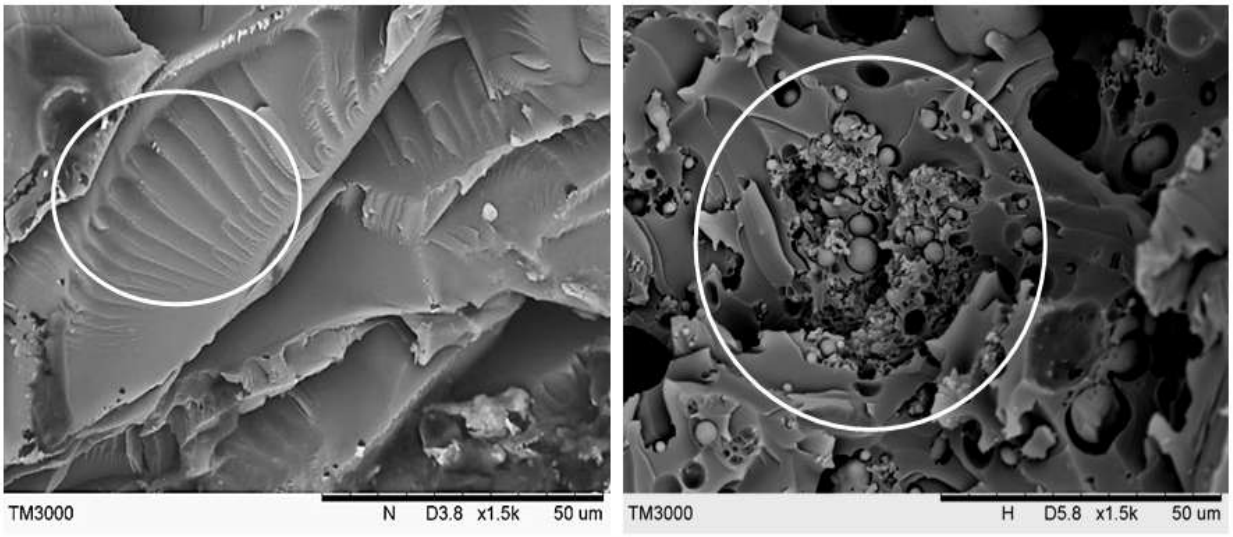

Fig 5; a) 0 wt% FA: Very small micro-size slip steps in epoxy deformation
b) 10 wt% FA- epoxy: shows agglomerating of FA and FA fracture

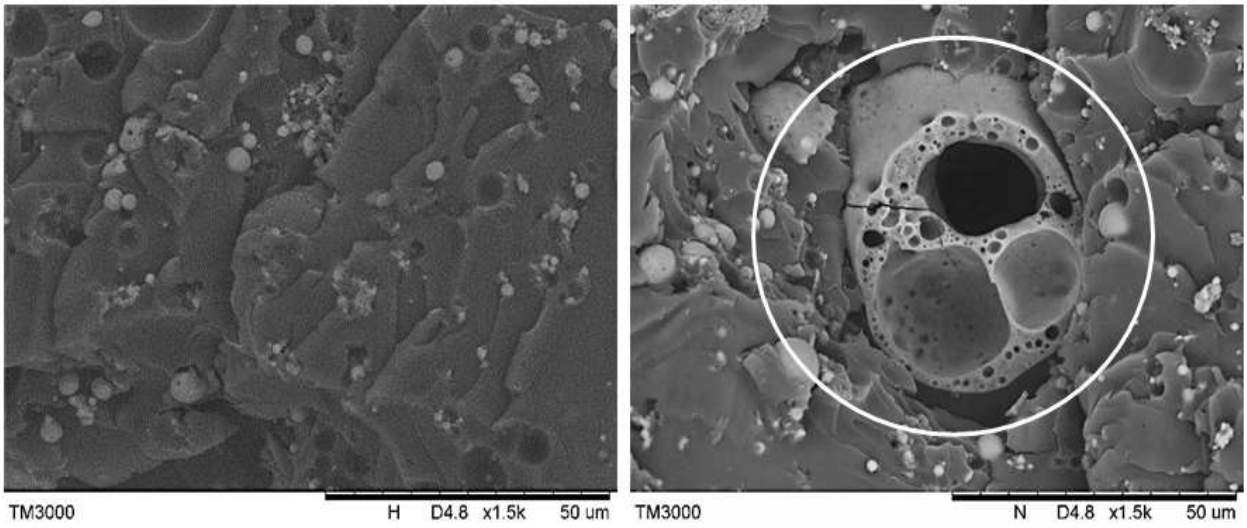

Fig 5; c) 20 wt% FA-epoxy composites showing even distribution of FA
d) 30 wt% FA: Shows fly epoxy - FA micro - cylinder shell formation and break

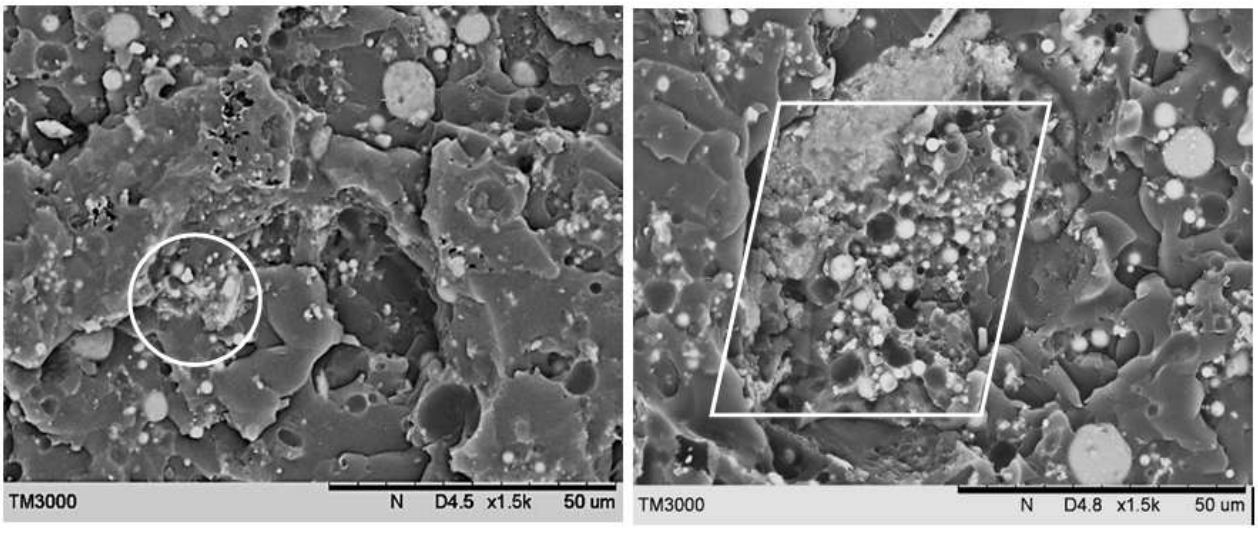

Fig 5; e) 40 wt% FA: shows small agglomeration
f) 50 wt% FA: shows substantial fly ash agglomeration

Fig 5; a, b, c, d, e, and f respectively showing SEM images of 0, 10, 20, 30, 40, and 50 wt% FA-epoxy composites 1500 magnification

At the magnification of 5000X (fig. 6), the following features were noted:

- Fig 6 a) shows evidence of some sub-micron shear lips in the epoxy [17].
- Figure 6 b) 10 wt% FA: shows grown crack with two fly ash particles visible, also shows that some of the fly ash particles are bonded to the matrix and the others are pulled out.
- Figure 6 c) 20 wt% FA individual FA particles in epoxies.
- Figure 6 d) 30 wt% FA: shows the debonding which happen with large particles rather than small particles. Fig 6 d) also shows the matrix stuck on fly ash surface particles which means that the FA particles have good/ excellent adherence to the epoxy matrix which furthermore approve that the interfacial adhesion is stronger than the epoxy resin strength. The good interfacial bonding would enhance the composite strength [18].
- Figure 6 e) 40 wt% FA: shows cenosphere FA fly ash particle snapped into half; beside it one can see the full grown crack with one fly ash particle visible.
- Figure 6 f) 50 wt% FA: shows that some of the fly ash particles are attached to the matrix and the others are pulled out.

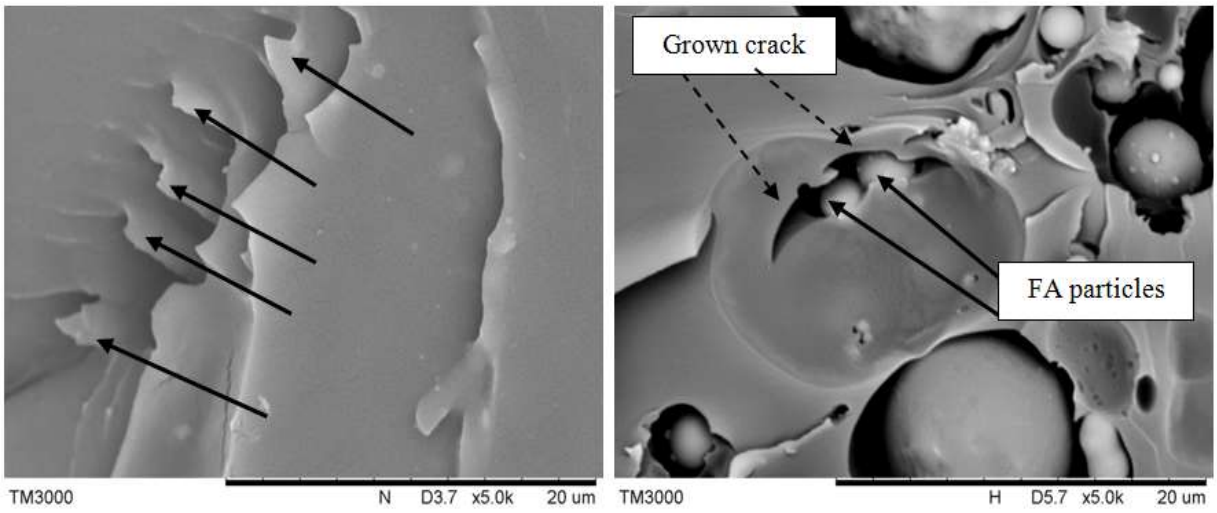

Fig 6 a) 0 wt% FA
b) 10wt% FA: Shows grown crack with two FA particles visible also shows that some of FA particles are bonded to the matrix and the others are pulled out

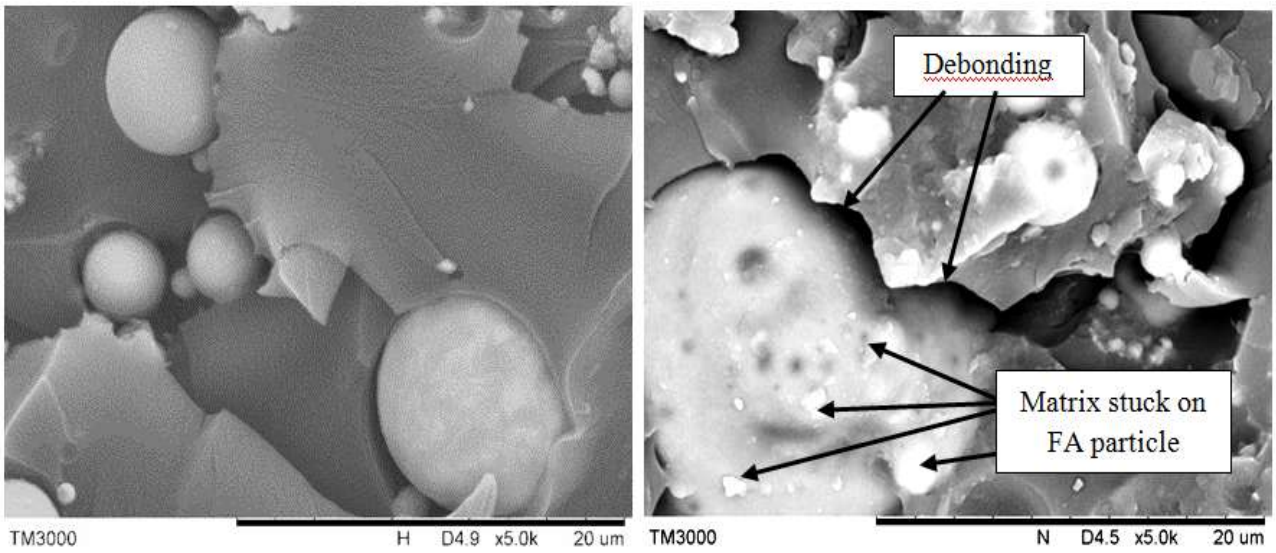

Fig 6c) 20 wt% FA showing individual FA particles in epoxies
d) 30 wt% FA: debonding which happen with large particles rather than small particles and shows also that the matrix stuck on the fly ash surface particles which give better strength to the composites

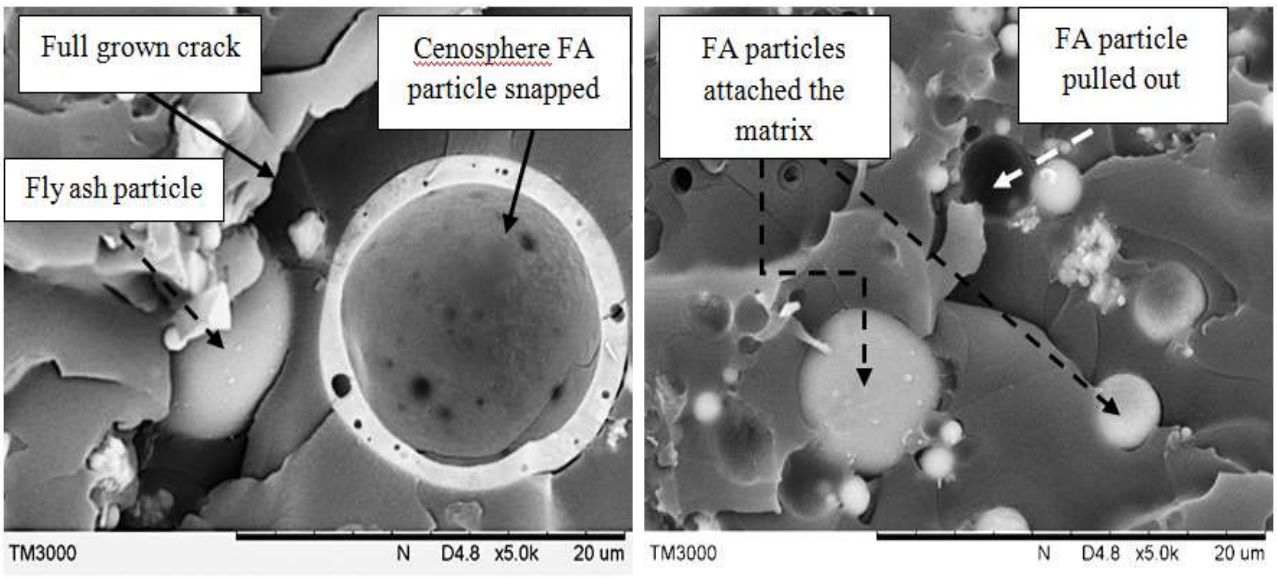

Fig 6 e) 40 wt% FA: cenosphere FA particle snapped into half which beside it one can see the full grown crack with one fly ash particle visible
f) 50 wt% FA: some of the fly ash particles are attached to the matrix and the others are pulled out

Fig 6: a, b, c, d, e, and f respectively showing SEM images of 0, 10, 20, 30, 40, and 50 wt% FA-epoxy composites 5000 magnification

At the magnification of 7000X (fig. 7), the following was noted:

- Figure 7 a) 0 wt% FA: shows 'micro -ductile' necking type deformation in the epoxy.
- Figure 7 b) 10 wt% FA: shows bond stretching between large FA particles and epoxy, also it can be seen that there are some residues of epoxy matrix still stuck to the FA particle. Both bond stretching and epoxy matrix sticking behaviours happen most likely because of plastic deformation that could lead to enhance the mechanical properties [19, 20].
- Figure 7 c) 20 wt% FA showing bonded full-moon type distribution in the epoxy matrix. It also appears that the FA particles are smooth (no epoxy matrix residues are stuck to the FA surface) which suggests that the interfacial bonding was weak [18].
- Figure 7 d) 30 wt% FA: shows some small FA particles are still bonded at the pull-out sites of larger FA particles.
- Figure 7 e) 40 wt% FA: shows matrix brittle fracture and adhering as fibril to a large FA.
- Figure 7 f) 50 wt% FA: shows one fly ash particle surrounded by epoxy from all sides.

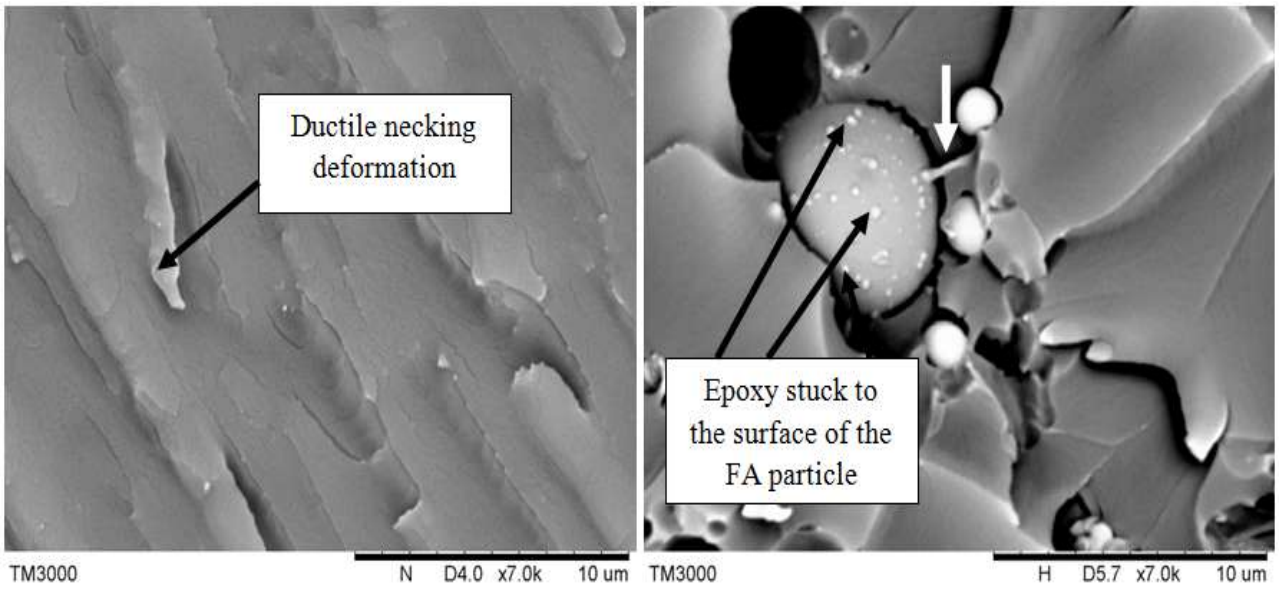

Fig 7; Left a) 0 wt% FA: 'ductile' necking type deformation in the neat epoxy
Right b) 10 wt% FA: shows bond stretching between large FA particles and epoxy

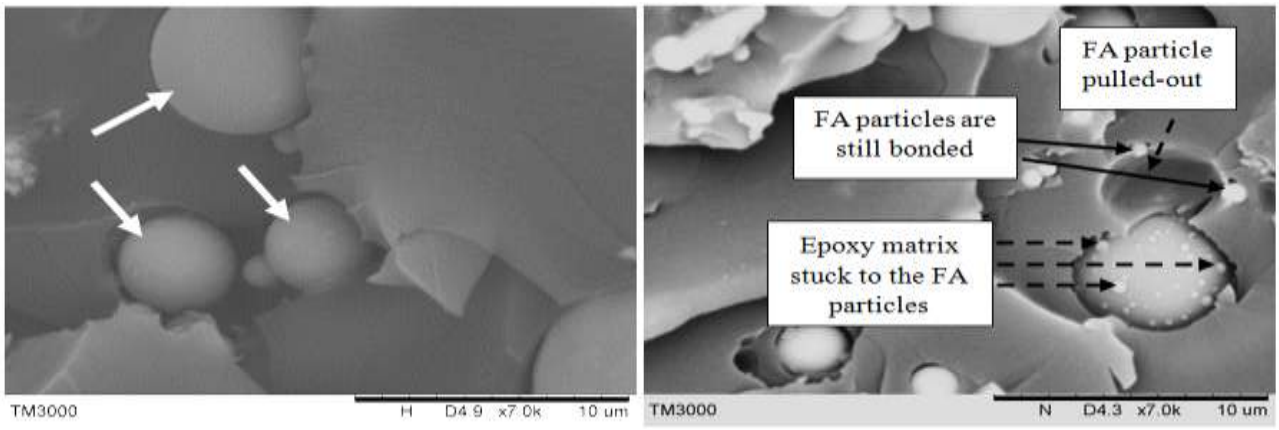

Fig 7; Left c) 20 wt% FA showing bonded full-moon type distribution in the epoxy matrix
Right d) 30 wt% FA: some small FA particles are still bonded at the pull - out sites of larger FA particles

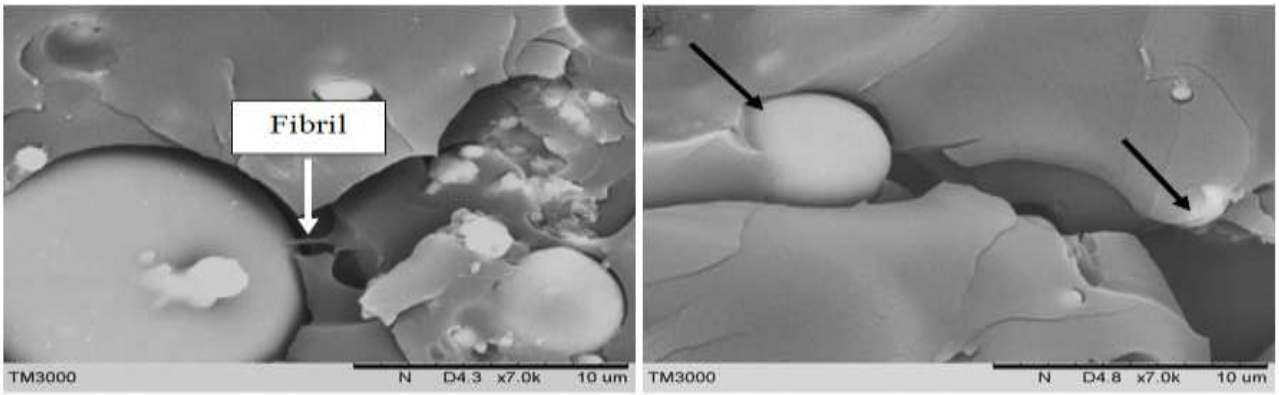

Fig 7; Left e) 40 wt% FA: matrix ductile fracture and adhering as fibril to a large FA
Right f) 50 wt% FA: two fly ash particles surrounded by epoxy from all sides

Fig 7; a, b, c, d, e, and f respectively showing SEM images of 0, 10, 20, 30, 40, and 50 wt% FA-epoxy composites 7000 magnification

3.2. FTIR of DGEBA

The FTIR spectrum of the as-received pure DGEBA resin after curing at 120°C for 2 hours is shown in fig. 8.
The FTIR spectrum for pure fly ash is also shown in fig. 8. The FTIR spectra for 20 wt% FA-epoxy and 40 wt% FA-epoxy composites are shown in fig. 10.

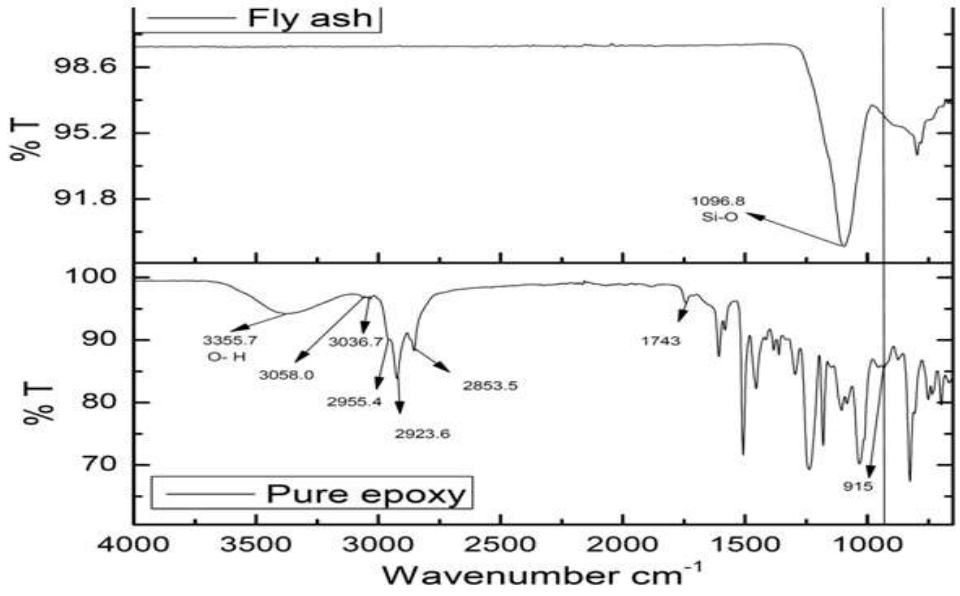

Figure 8: FTIR for the raw fly ash and also pure epoxy as cured at 120 ºC /2 hrs

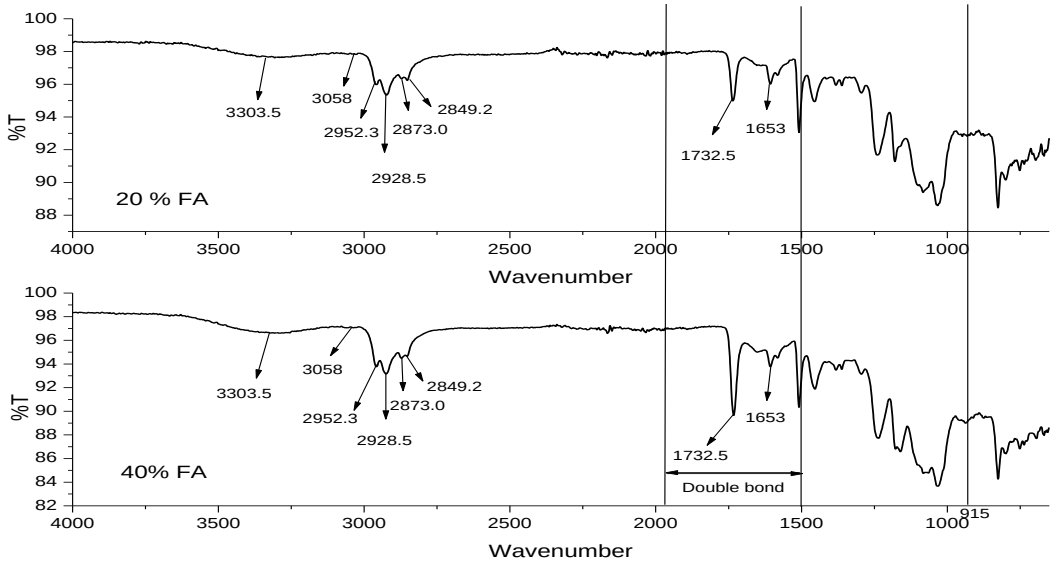

Figure (9): Composites FTIR comparison graphs for 20 wt% FA-epoxy & 40 wt% FA-epoxy

For the FTIR spectrum of cured pure epoxy (fig. 8), the following was noted:

1. A) 915 cm^{-1} represents epoxy group –C<O
   B) 305 cm^{-1} represents C-H stretching in epoxy group e ring.
   So A and B are characteristic peaks of epoxy representing extent of crosslinking taking place in the fabricated sample.
2. 3036 cm^{-1} is a C-H stretching peak aromatic ring.
3. Several peaks absorbed in the range 1550 - 1900 cm^{-1} represent double bond C=C aromatic ring present in the epoxy polymer.
4. The broad peak observed at 3355 cm^{-1} represents polymer O-H stretching.

For the FTIR spectrum of as-supplied fly ash (fig. 8), the following was noted:

1. The absence of the peak 3355 cm^{-1} indicates that was there was no significant moisture content of the FA.
2. The Very strong peak at 1096 cm^{-1} reveals the presence of Si-O bond representing enrichment in SiO_2 or Silicon Oxide which is a significant content of fly ash.

For the FTIR spectrum of 20 wt% FA-epoxy and 40 wt% FA-epoxy (fig 9), the following was noted:

- FTIR spectra for the two FA-epoxy composites which have similar peaks.
- FTIR for both composites does not show any peak at 915 cm^{-1} which indicates that addition of FA does not obstruct the crosslinking of the DGEBA. Same behaviour is observed at 3056 cm^{-1}.
- 1732 cm^{-1} in both composites belongs to carboxyl group (C=O), the impurities present in FA react with secondary alcohol present in the epoxy and forms carboxyl group.
- Second new peak for both composites observed at 1653 cm^{-1} which represent O-H bending in the composite. This provides an idea of increasing moisture content in both composites presumably indicating epoxy as the source of moisture.

From the results it can be observed that

- No moisture content is found using FTIR of the used FA.
- Addition of FA to the epoxy gives indication of feasible bonding as peak 915 cm^{-1} has disappeared.

3.3. Secondary Ion Mass Spectrometry (SIMS) for 20% FA:

The figures were taken after 5 minutes restering. The dimensions of the tested zone was 250 μm width, 200 μm length
Following our research with SIMS in Ref (9)

- SIMS bombardment area at 200 magnification is given in figure 11, whilst the details of SIMS are given in figures 12 a – 12 g.
- The corresponding EDS map and the elemental peaks are given in figures 13 and 14.

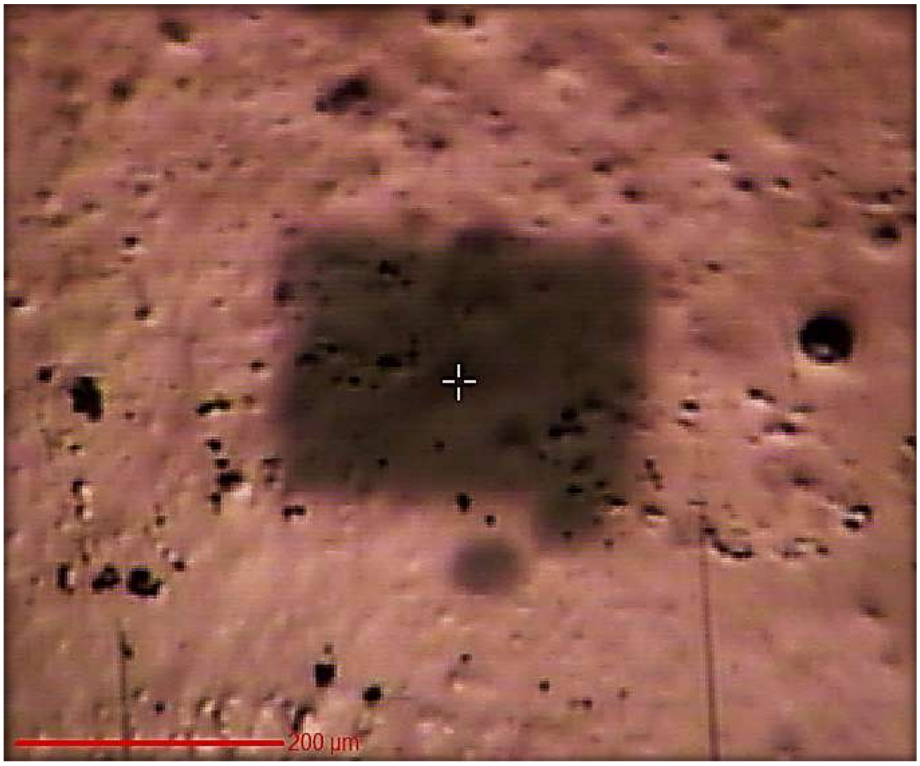

Fig 11: SIMS for 20% FA at higher magnification

SIMS results 20%FA

- A pine cone type agglomeration can be noticed in figures 12 a – 12 c which is related to the Ca , K and Mg respectevely, which all have approximately 100 µm width, but the most imporant thing noticed is the three elemental agglomerations happening in the same area with different concentrations showing that K have the higher agglomerated concentration and Mg have the lower one depending on the strength of the colour of the agglometated area.
- In figures 12d, 12f and 12g: Al, O, and Mn have the most uniform distribution of all elements.
- Figure 12e shows that in the middle and lower parts of the sample, there is much less yet uniform distribution of Si whilst in the top part there is more concentration of Si element.
- The respective ions are converted in to scales of black to red. It is immediately apparent that there are well defined blue/ green/ red bands .

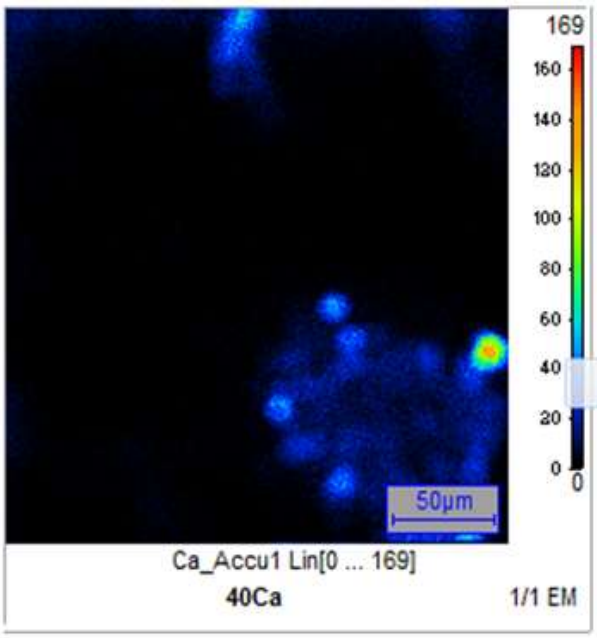

Fig 12a: SIMS result for Ca

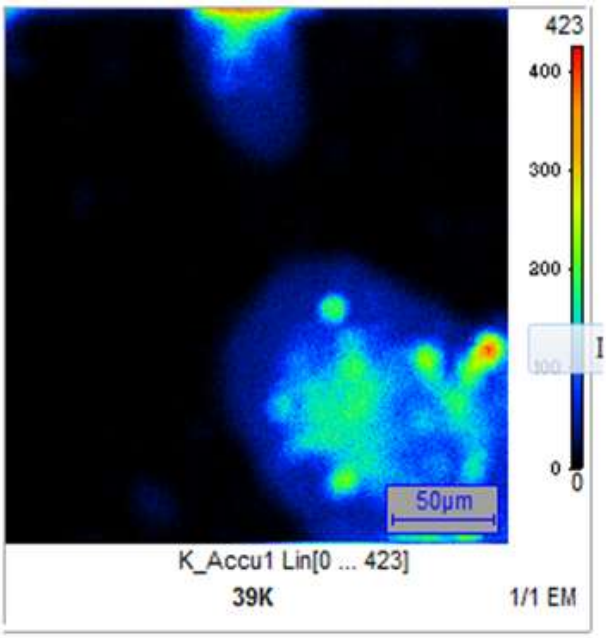

Fig 12b: SIMS result for K

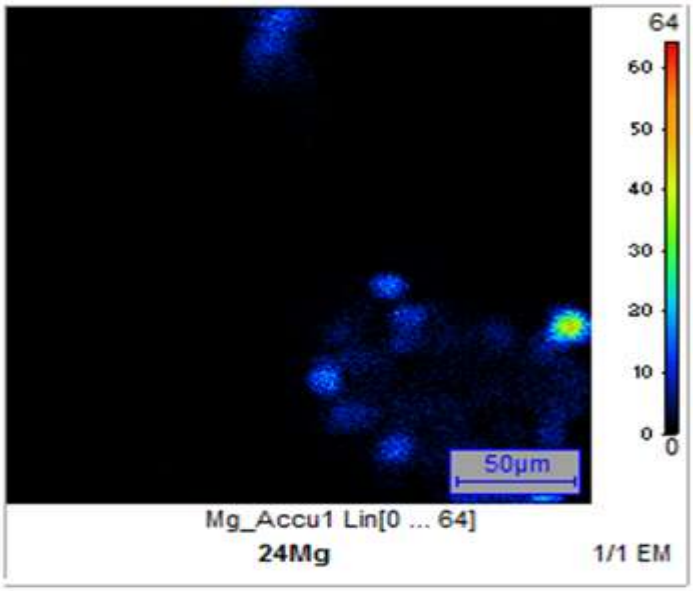

Fig 12c: SIMS result for Mg

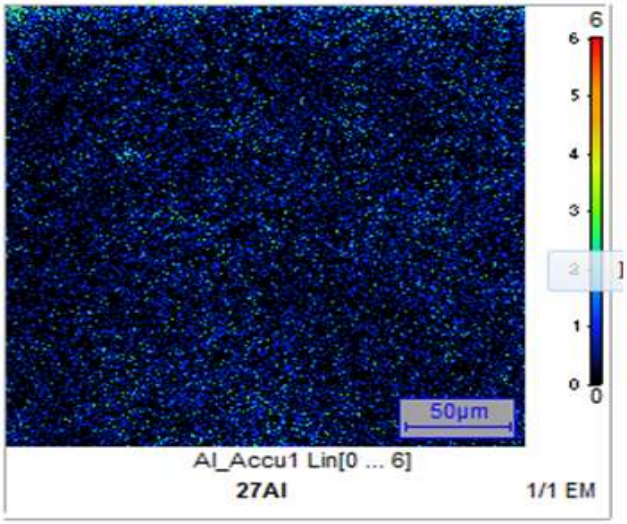

Fig 12d: SIMS result for Al

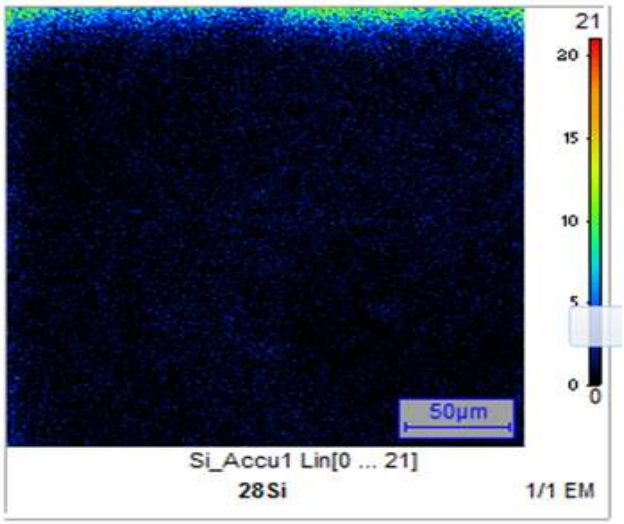

Fig 12e: SIMS result for Si

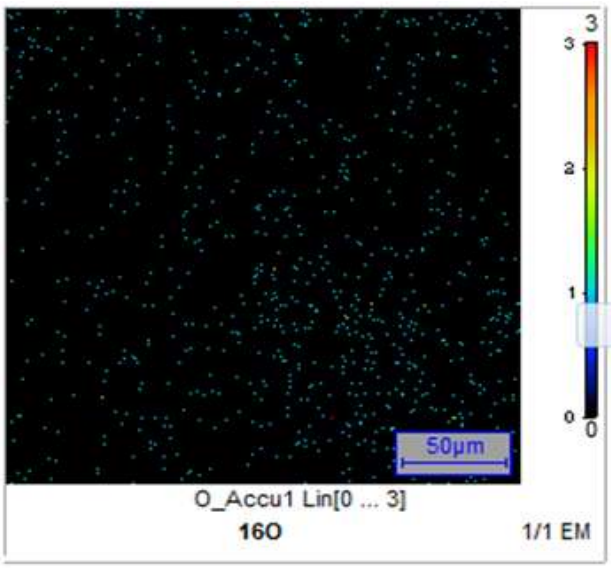

Fig 12f: SIMS result for O

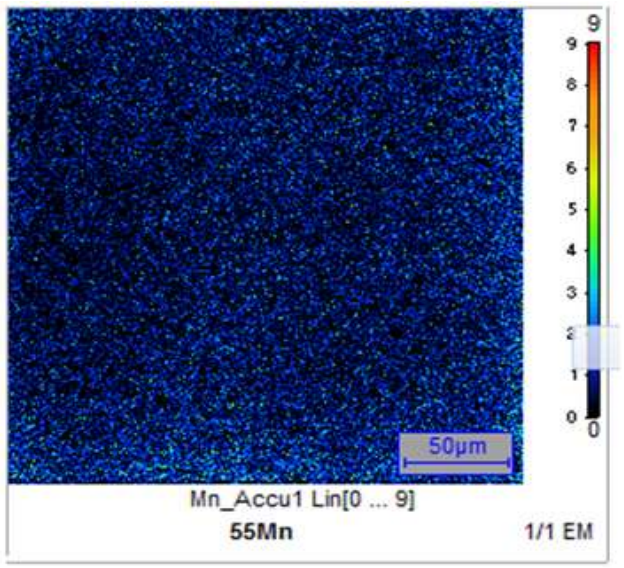

Fig 12g: SIMS result for Mn

3.4. EDS Micrograph for 20% FA:

The EDS results for the area enclosed in the SEM of figure 13 are shown in Fig 14.

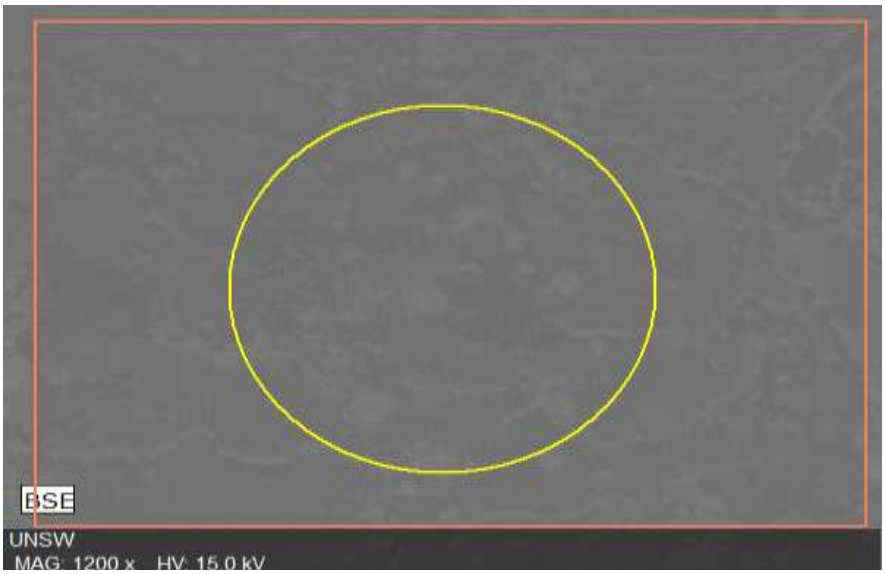

Fig 13: SEM micrograph for 20% FA-epoxy

EDS results for 20% FA:

In figure 14: only C and O can be found, but no Mn, Fe, Ca and S.

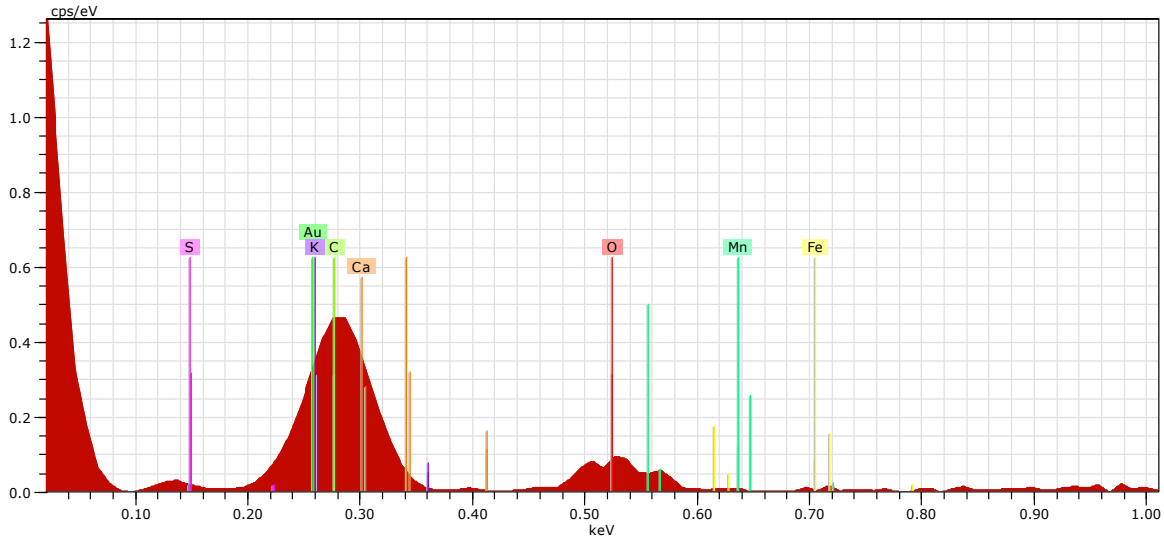

Fig 14: EDS spectra for 20% FA- epoxy

Table 1 : Repreentative SIMS and EDS results of 20% FA- epoxy

Elements identified	SIMS	EDS
Si	Yes	No
Mg	Yes	No
K	Yes	No
Al	Yes	No
Ca	Yes	No
Mn	yes	No
O	Yes	Yes
C	No	Yes

4. SUMMARY

- As received Fly ash – epoxy composites were fabricated using DGEBA epoxy and crosslinking agent cycloaliphatic polyamine cured at 120 ^{o}C for 2 hours - using an as-received class F fly ash in the proportion 0, 10, 20, 30, 40 and 50 weight %.
- SEM studies of the tensile fracture surfaces of the compositions of as-received fly-ash epoxy composites showed the following important observations:

  - Overall, fly ash has been homogeneously mixed with the epoxy.
  - There is minimal amount of voids seen on fracture surfaces
  - Good bonding was found between the fly ash and the epoxy.
  - Although at higher magnifications, evidence of debonding and pull-out are found in the composites which happen more with the large rather than small fly ash particles but the presence of epoxy matrix – could be seen at higher magnification- on the FA particle surface indicating better adhesion between Epoxy and FA which most likely enhanced energy absorption by the larger particles, 10 um and above [20].
  - Some of the SEM micrographs strongly show that the matrix adheres to the fly ash surface particles which expectedly would give better strength to the composites.

- FTIR studies show definitive chemical bonding between the epoxy and as-received fly ash- which is an interesting and positive result:

  - No moisture content is found using FTIR of the used FA.
  - Addition of FA to the epoxy gives indication of feasible bonding as peak 915 cm^{-1} has disappeared.

- SIMS of the selected composite i.e. 20% FA- epoxy composite gives better results comparing to EDS that detect such elements like Ca, K, Mg, Al, Si, O, and Mn while the EDS could just detect C and O elements. Also SIMS gives distribution of Ca, K, Mg, Al, Si, O, and Mn elements in the matrix.

From commercial point of view, as received fly ash waste was found very attractive as an additive in epoxy resin up to 50 % reducing the cost of the used matrix by about 50 % and achieving a range of superior properties.

REFERENCES

[1]. The American Coal Ash Association (ACAA) > About Coal Ash > What are CCPs? > Fly Ash
[2]. Raask E. Cenospheres in pulverized-fuel ash. J Inst Fuel 1968; 41(332): 339–44.
[3]. McKerall, W.C., Ledbetter W.B., and Teague D. J., 1982 Analysis of Fly Ashes Produced in Texas. Texas Transportation Institute, Research Report No. 240-1, Texas A&M, University, College Station, Texas.
[4]. Manoj Singla and Vikas Chawla ,Journal of Minerals and Materials Characterization and Engineering ,Vol.9,No.3,pp.199-120.2010"Mechanical Properties of Epoxy Resin-Fly Ash Composite"
[5]. Wikipedia. "Epoxy", 25 April 2012. http://en.wikipedia.org/wiki/Epoxy.
[6]. "Epoxy Resins". http://pslc.ws/macrog/epoxy.htm
[7]. "Crosslinking" 2005. http://pcls.ws/macrog/xlink.htm
[8]. http://www.wisegeek.com/what-is-epoxy-resin.htm
[9]. Shahad Ibraheem, Sheila. Devasahayam, Owen Standard, Sri Bandyopadhyay: "Use of Secondary Ion Mass Spectrometry (SIMS) to identify Fly Ash Mineral spatial and particulate distribution in Epoxy Polymer" International Journal of Minerals Processing, 142 (2015) 139 - 146 http://dx.doi.org/10.1016/j.minpro.2015.04.025
[10]. S.M. KULKARNI, KISHORE," Studies on fly ash –filled epoxy-cast slabs under compression, Journal of applied polymer science, Volume 84, Issue 13, pages 2404– 2410, 2001.
[11]. S.M. KULKARNI, KISHORE," Studies on fly ash –filled epoxy-cast slabs under compression ". India, 18 August 2001.
[12]. Knoll, Max (1935). "Aufladepotentiel und Sekundäremission elektronenbestrahlter Körper". Zeitschrift für technische Physik **16**: 467–475.
[13]. Von Ardenne M. "Improvements in electron microscopes". GB 511204, convention date (Germany) 18 February 1937
[14]. Wikipedia, "Scanning electron microscope". https://en.wikipedia.org/wiki/Scanning_electron_microscope.
[15]. S Bandyopadhyay, Gellert, E.P., Silva, V.M. and Underwood, J.H. (1989) "Microscopic Aspects of Failure and Fracture in Cross-Ply Fibre Reinforced Composite Laminates", J. Composite Materials, Vol 23(12), pp. 1216-1231
[16]. S Bandyopadhyay (1990) "Review of the Microscopic and Macroscopic Aspects of Fracture Behaviour of Unmodified and Modified Epoxy Resins", Materials Science and Engineering, A125, pp. 157-184.
[17]. http://mmrc.caltech.edu/FTIR/FTIRintro.pdf
[18]. C. Kanchanomaia, S. Rattananon, M. Soni, "Effects of loading rate on fracture behaviour and mechanism of thermoset epoxy resin" Polymer Testing 24 (2005). Pages 886–892.
[19]. Mohammed Kamal Hosain. "Scanning electron microscopy study of fibre reinforce polymeric nanocomposites" 2012. Pages 731-744.
[20]. M.K.Hossain 2011, Mohammed, Mohamed H.Gabr, Kazuya Okubo, and Toru Fujii, Pages 250-261"Mechanical and morphology properties of cellulose nanocomposites" Handbook of polymer nanocomposites. proswssing, performance and application volume C: Polymer nanocomposites of Cellulose nanoparticles, volume 3, 1 Dec 2014
[21]. María González González, Juan Carlos Cabanelas and Juan Baselga. Applications of FTIR on epoxy resins – identification, monitoring the curing process, phase separation and water uptake. Pages 262-283.